On the dynamics of polymer melts: Contribution of Rouse and bending modes

EUROPHYSICS LETTERS 15 February 1999

Europhys. Lett., **45** (4), pp. 488-494 (1999)

On the dynamics of polymer melts: Contribution of Rouse and bending modes

L. Harnau, R. G. Winkler and P. Reineker

Abteilung Theoretische Physik, Universität Ulm - 89069 Ulm, Germany

(received 14 September 1998; accepted in final form 11 December 1998)

PACS. 61.25.Hq– Macromolecular and polymer solutions; polymer melts; swelling.

Abstract. – The influence of molecular stiffness on the dynamic properties of polymer melts is investigated analytically. It is shown that the relaxation times characterizing the internal dynamics of the polymer chains exhibit a crossover from Rouse to bending modes with increasing mode number. As a consequence the mean square displacement of monomers and the dynamic structure factor are strongly influenced by the molecular stiffness. The comparison of both equilibrium and dynamical properties of n-alkane chains in a melt with recent molecular dynamics simulations and neutron scattering experiments exhibits excellent agreement.

The dynamics of unentangled polymer melts is usually considered within the Rouse model [1-5] which describes the polymer chains as random walks. Although many predictions of the Rouse model are in agreement with experimental results, recently published neutron scattering measurements and molecular dynamics simulations [6-9] reveal severe deficiencies of the Rouse model in describing various dynamical properties of unentangled polymer melts. The relaxation times of the normal modes characterizing the dynamics of the polymer chains, the mean square displacement of the monomers and the dynamic structure factor deviate from the Rouse model prediction. In this article we demonstrate that with a semiflexible chain model [10-12], which is an extension of the Rouse model taking into account molecular stiffness, neutron scattering measurements [7] and simulation data [6] of n-$C_{100}H_{202}$ alkane chains in a melt can be described very well. The investigations demonstrate the importance of a theoretical approach for the dynamics of polymers in a melt which includes molecular stiffness.

In our calculations the polymer chain is described by a continuous, differentiable space curve $\mathbf{r}(s)$, where s indicates distances along the chain. The partition function of this chain of contour length L is calculated using the maximum-entropy principle together with constraints on the contour length and on the curvature of the chain [10]:

$$Z = \int \exp\left[-\frac{3p}{2}\int_{-\frac{L}{2}}^{\frac{L}{2}} \left(\frac{\partial \mathbf{r}(s)}{\partial s}\right)^2 \mathrm{d}s - \frac{3}{4}\left(\frac{\partial \mathbf{r}(\frac{L}{2})}{\partial s}\right)^2 - \frac{3}{4}\left(\frac{\partial \mathbf{r}(-\frac{L}{2})}{\partial s}\right)^2 - \right.$$
$$\left. -\frac{3}{8p}\int_{-\frac{L}{2}}^{\frac{L}{2}} \left(\frac{\partial^2 \mathbf{r}(s)}{\partial s^2}\right)^2 \mathrm{d}s \right] \mathcal{D}^3 x\,, \qquad (1)$$

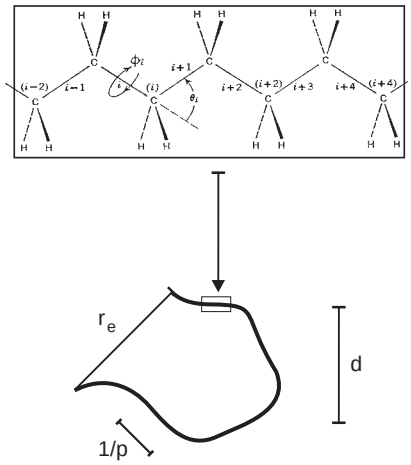

Fig. 1. – Continuous chain model for n-$C_{100}H_{202}$ alkane chains (contour length $L = 12.57\,\mathrm{nm}$). The end-to-end distance and the persistence length are given by $r_\mathrm{e} = 3.94\,\mathrm{nm}$ and $1/(2p) = 0.65\,\mathrm{nm}$, respectively. The length $d = 2\pi/q$ corresponds to a scattering vector $q = 2\,\mathrm{nm}^{-1}$ used in neutron scattering experiments.

where $1/(2p)$ is the persistence length. The first three terms in the exponent characterize a flexible chain. The last term represents the bending energy, which accounts for the molecular stiffness. Equilibrium properties of our model, like the mean square radius of gyration, the mean square end-to-end distance, and the correlation of tangent vectors are identical with those of the Kratky-Porod wormlike chain [10].

The n-$C_{100}H_{202}$ alkane chains considered in this article are characterized by the contour length $L = 12.57\,\mathrm{nm}$ given by the end-to-end distance in the all-trans conformation. The persistence length of an alkane chain in a melt at temperature $T = 509\,K$ is not known exactly. We use $1/(2p) = 0.65\,\mathrm{nm}$ in accordance with the predictions of Yamakawa [13]. It follows that the calculated radius of gyration $r_g = 1.53\,\mathrm{nm}$ and the end-to-end distance $r_\mathrm{e} = 3.94\,\mathrm{nm}$ agree with the simulation data [6]. Furthermore, with the same persistence length it is also possible to describe equilibrium properties of n-$C_{44}H_{90}$ alkane chains [14] by means of the semiflexible chain model. Figure 1 shows a schematic presentation of the continuous chain model for n-$C_{100}H_{202}$ alkane chains. Because of the hindered rotation of the individual chemical bonds, the chain no longer follows random walk statistics on length scales comparable with the persistence length. The local contour tends to persist in a given direction. The molecular stiffness is considered from the macroscopic perspective, *i.e.*, with a view of alkane chains as uniform elastic chains. This view does not imply that microscopic details are unimportant. Rather it is based on the belief that microscopic models, which incorporate the details of local conformations and dynamics, will lead to the same stiffness parameter that is obtained through studies of long-range chain configurations.

The dynamics of polymer chains in a melt is formulated in terms of a formally exact generalized Langevin equation using a projection operator method [12]. The polymer chain positions and velocities are chosen as the primary slow variables. Because the n-$C_{100}H_{202}$ alkane chains are shorter than the entanglement length, intermolecular correlations are assumed to fluctuate on a shorter time scale than intramolecular correlations and the following Langevin equation

along with the boundary conditions for free chain ends are obtained [11,12]

$$\gamma\frac{\partial}{\partial t}\mathbf{r}(s,t) - 3k_{\mathrm{B}}Tp\frac{\partial^2}{\partial s^2}\mathbf{r}(s,t) + \frac{3k_{\mathrm{B}}T}{4p}\frac{\partial^4}{\partial s^4}\mathbf{r}(s,t) = \mathbf{f}(s,t)\,, \tag{2}$$

$$\left[p\frac{\partial}{\partial s}\mathbf{r}(s,t) - \frac{1}{4p}\frac{\partial^3}{\partial s^3}\mathbf{r}(s,t)\right]_{\pm\frac{L}{2}} = 0\,, \tag{3}$$

$$\left[\frac{\partial}{\partial s}\mathbf{r}(s,t) \pm \frac{1}{2p}\frac{\partial^2}{\partial s^2}\mathbf{r}(s,t)\right]_{\pm\frac{L}{2}} = 0\,. \tag{4}$$

γ is the friction constant per unit length of the polymer chains and $\mathbf{f}(s,t)$ is a stochastic force (white noise). The frictional force results from irreversible short time viscous processes. The second and third terms in eq. (2) describe intramolecular forces which follow from the identification of the exponent in the partition function (1) with the intramolecular potential energy of the system (multiplied by $1/k_{\mathrm{B}}T$). An expansion of the position vector

$$\mathbf{r}(s,t) = \sum_{l=0}^{\infty}\boldsymbol{\chi}_l(t)\psi_l(s)\,, \tag{5}$$

in terms of the eigenfunctions $\psi_l(s)$ (eqs. (2.22)–(2.24) of ref. [11]) of the corresponding eigenvalue equation

$$\frac{\gamma}{\tau_l}\psi_l(s) = 3k_{\mathrm{B}}Tp\frac{\partial^2}{\partial s^2}\psi_l(s) - \frac{3k_{\mathrm{B}}T}{4p}\frac{\partial^4}{\partial s^4}\psi_l(s)\,, \tag{6}$$

yields the following equation for the time correlation function $\langle\boldsymbol{\chi}_l(t)\cdot\boldsymbol{\chi}_l(0)\rangle$ of the amplitude $\boldsymbol{\chi}_l(t)$:

$$\frac{\partial}{\partial t}\left\langle\boldsymbol{\chi}_l(t)\cdot\boldsymbol{\chi}_l(0)\right\rangle = -\frac{1}{\tau_l}\left\langle\boldsymbol{\chi}_l(t)\cdot\boldsymbol{\chi}_l(0)\right\rangle\,, \tag{7}$$

with the solution

$$\left\langle\boldsymbol{\chi}_l(t)\cdot\boldsymbol{\chi}_l(0)\right\rangle = \frac{3k_{\mathrm{B}}T}{\gamma}\tau_l\exp\left[-\frac{t}{\tau_l}\right]\,. \tag{8}$$

τ_l are the relaxation times of the normal mode analysis discussed in detail in ref. [11]. The amplitudes of different intramolecular modes are uncorrelated and the equipartition law is fulfilled. The first 10 relaxation times are plotted in fig. 2 as a function of pL. For relaxation times $\tau_l\,, l > 1$, three regimes can be distinguished. In the limit of $pL \gg l\pi/2$ the relaxation times are proportional to L^2 and vary as l^{-2} representing the well-known Rouse relaxation times [4]. In the limit of $pL \ll l\pi/2$ the relaxation times are proportional to L^4 and exhibit the dependence $(2l-1)^{-4}$ on the mode number, as known for the bending modes of the model of Aragon and Pecora [15], resulting in a wider distribution of the relaxation times. In the intermediate regime both bending and Rouse modes contribute to the relaxation times. The maximum of $\tau_l(pL)$ shifts continuously to larger pL values with increasing l. This simply reflects the fact that any real polymer looks increasingly rigid on smaller length scales. Therefore, the model yields a crossover from Rouse to bending modes with increasing mode number on small length scales even for very flexible chains (pL large) due to molecular stiffness. The first relaxation time τ_1 is proportional to L^3 in limit of very stiff chains ($pL \to 0$).

Figure 3 displays the first 10 calculated relaxation times τ_l/τ_2 for n-$C_{100}H_{202}$ alkane chains ($pL = 9.67$) together with simulation data of Paul *et al.* [6] as a function of the inverse square of the mode number l. The dotted line corresponds to the Rouse model prediction $\tau_l \sim 1/l^2$.

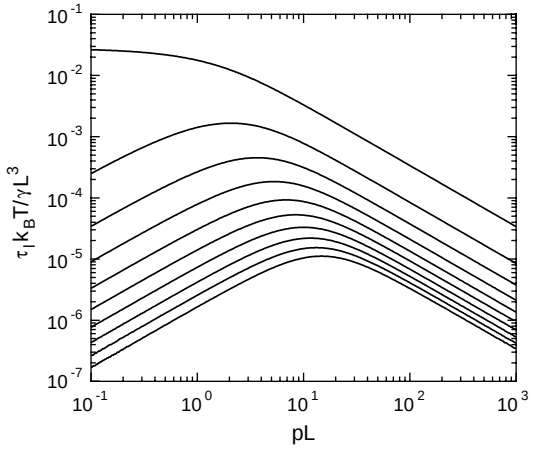

Fig. 2

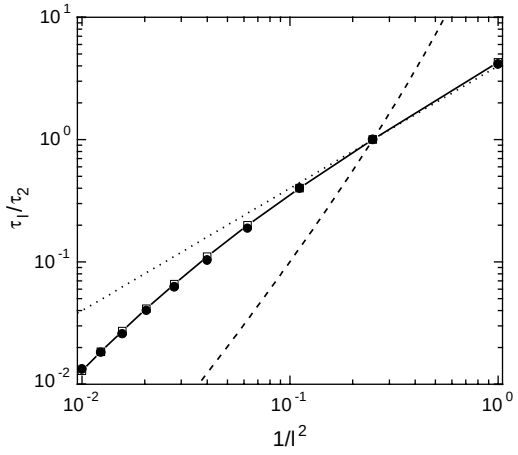

Fig. 3

Fig. 2. – The first 10 relaxation times τ_l ($l = 1, ..., 10$) as function of pL. Mode number l increases from top to bottom.

Fig. 3. – Computed relaxation times τ_l/τ_2 for n-$C_{100}H_{202}$ alkane chains as a function of the Rouse scaling variable $1/l^2$ (open squares and solid line). Filled circles display simulation data [6]. The dotted and the dashed line display the relations $\tau_l \sim 1/l^2$ and $\tau_l \sim 1/(2l-1)^{-4}$, respectively.

The dashed line displays the relation $\tau_l \sim 1/(2l-1)^{-4}$ valid for bending modes. As is obvious from the figure the calculated relaxation times are in excellent agreement with the simulation data. Only the first two relaxation times follow the Rouse scaling prediction. The higher modes systematically deviate from the Rouse model prediction. Furthermore, an analysis in terms of bending modes only yields also an incorrect l-dependence of the relaxation times. Hence, using either bending modes only or Rouse modes only fails to describe the experimental data. Consequently, it is necessary to include both, as suggested by our theoretical approach.

The dynamics of polymer chains is often characterized by various mean square displacements. Here we investigate the mean square displacement $g_1(t)$ for the central monomer. Using the transformation (6) and the correlation functions (8) this quantity is given by

$$g_1(t) = \left\langle (\mathbf{r}(0,t) - \mathbf{r}(0,0))^2 \right\rangle$$
$$= \frac{6k_B T}{\gamma L} \left(t + L \sum_{l\,\mathrm{odd}}^{\infty} \tau_l \psi_l^2(0) \left(1 - \exp\left[-\frac{t}{\tau_l} \right] \right) \right) . \tag{9}$$

In fig. 4 we present $g_1(t)$ (solid line) together with simulation data of n-$C_{100}H_{202}$ alkane chains in a melt [6, 16]. The dotted line corresponds to the asymptotic $t^{1/2}$-dependence of $g_1(t)$ according to the Rouse model [4]. The dashed line displays the relation $g_1(t) \sim t^{3/4}$ valid if only bending modes are considered [17]. Figure 4 exhibits good agreement between our model calculations and the simulation data. The observed behavior is a manifestation of the molecular stiffness of the alkane chains. The deviations from the $t^{1/2}$-dependence are obvious. These deviations are due to the relaxation spectrum presented in fig. 3. The $t^{1/2}$-dependence of $g_1(t)$ is valid only in the case when the relaxation times follow the scaling prediction of the Rouse model.

An analysis in terms of bending modes also yields an incorrect time dependence of the

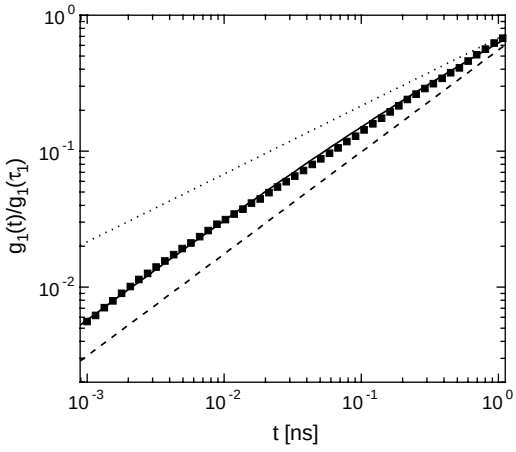

Fig. 4

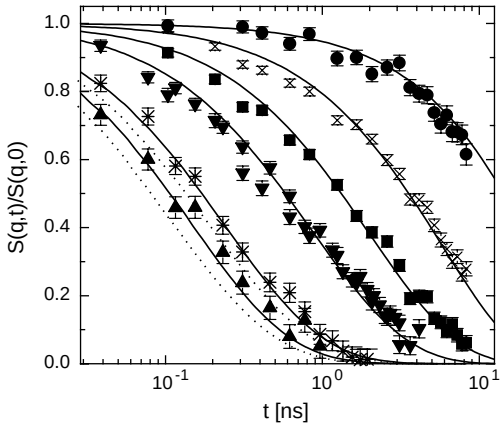

Fig. 5

Fig. 4. – Computed mean square displacement for the central monomer (solid line) together with simulation data (filled squares [6, 16]) of n-$C_{100}H_{202}$ alkane chains in a melt. The dotted and the dashed line display the power laws $g_1(t) \sim t^{1/2}$ and $g_1(t) \sim t^{3/4}$, respectively.

Fig. 5. – Computed dynamic structure factor $S(q,t)/S(q,0)$ (solid lines) for various scattering vectors q according to eqs. (11) and (12) together with experimental results for alkane chains in a melt (circles, $q = 0.55\,\mathrm{nm}^{-1}$; crosses, $q = 1\,\mathrm{nm}^{-1}$; squares, $q = 1.4\,\mathrm{nm}^{-1}$; down triangles, $q = 1.8\,\mathrm{nm}^{-1}$; stars, $q = 2.6\,\mathrm{nm}^{-1}$; up triangles $q = 3\,\mathrm{nm}^{-1}$) [7]. The two dotted lines represent the Rouse model calculations for $q = 2.6\,\mathrm{nm}^{-1}$ and $q = 3\,\mathrm{nm}^{-1}$, respectively.

mean square displacement. The power law $g_1(t) \sim t^{3/4}$ has been observed for rather rigid f-actin [18].

In dynamic light scattering experiments the dynamic structure factor

$$S(\mathbf{q},t) = \frac{1}{L^2} \int_{-\frac{L}{2}}^{\frac{L}{2}} \int_{-\frac{L}{2}}^{\frac{L}{2}} \mathrm{d}s\,\mathrm{d}s'\ \langle \exp\left[i\mathbf{q}\cdot(\mathbf{r}(s,t)-\mathbf{r}(s',0))\right]\rangle \tag{10}$$

is studied as a function of time and scattering vector $\mathbf{q}$. Recently, Paul *et al.* [7] investigated the dynamic structure factor of n-$C_{100}H_{202}$ alkane chains in in a melt by means of neutron spin echo spectroscopy and molecular dynamics simulations. As shown in fig. 2 of ref. [7] a comparison of the experimental data with a Rouse model calculation exhibits severe deviations. In particular at large scattering vectors a slower relaxation of the dynamic structure factor was found than predicted by the Rouse model. Here we compare our model calculations with the experimental data. Using the fact that the distribution of $(\mathbf{r}(s,t)-\mathbf{r}(s',0))$ is Gaussian for our chain model we obtain with the help of the transformation (6) and the time correlation function (8)

$$S(\mathbf{q},t) = \frac{1}{L^2} \int_{-\frac{L}{2}}^{\frac{L}{2}} \int_{-\frac{L}{2}}^{\frac{L}{2}} \mathrm{d}s\,\mathrm{d}s'\ \exp\left[-\frac{q^2}{6} g(s,s',t)\right], \tag{11}$$

where

$$g(s,s',t) = \frac{6k_{\mathrm{B}}T}{\gamma L}\left(t + \frac{L}{2}\sum_{l=1}^{\infty}\tau_l\left(\psi_l^2(s) + \psi_l^2(s') - 2\psi_l(s)\psi_l(s')\exp\left[-\frac{t}{\tau_l}\right]\right)\right), \qquad (12)$$

and $q = |\mathbf{q}|$. Figure 5 displays the computed dynamic structure factor according to eqs. (11) and (12) together with experimental data for alkane chains in a melt [7]. As is obvious from a comparison with fig. 2 of ref. [7], our analytical approach is in closer agreement with the experimental data than the Rouse model calculations. The deviations of the Rouse model calculations at large scattering vectors (dotted lines in fig. 5) are due to the neglect of molecular stiffness, which has to be taken into account for large scattering vectors $q > 2\,\mathrm{nm}^{-1}$. With increasing scattering vector more internal modes become important in the evaluation of the dynamic structure factor according to eqs. (11) and (12). On spatial length scales comparable with the persistence length, internal modes with mode numbers $l > 2pL/\pi$ dominate the relaxation of the dynamic structure factor. As was discussed earlier and is apparent from fig. 2 and fig. 3 these modes do not follow the Rouse scaling prediction. Hence the calculated dynamic structure factor decays slower than the Rouse model prediction in agreement with the experimental data. Thus, for an adequate description of the dynamic structure factor of alkane chains in a melt a semiflexible chain model is essential. If improved experimental scattering data yield deviations from our semiflexible-chain-model calculations, a more appropriate description of the dynamics of alkane chains is required and possibly intermolecular correlations have to be considered.

Finally, we like to mention that the experimental data cannot be described by the dynamic structure factor in the pure bending limit [19-21]. Considering bending modes only the dynamic structure factor is a universal function of only the combination $q^{\frac{8}{3}}t$. This scaling behaviour has been confirmed experimentally for f-actin [20, 21]. However, for n-$C_{100}H_{202}$ alkane chains we found a crossover from a q^4t (Rouse modes) to a $q^{\frac{8}{3}}t$ (bending modes) scaling with increasing scattering vector.

We hope that this investigation and our previous study [11] will give a deeper insight into the dynamics of polymers in a melt. It would be interesting to check the predictions of our model calculations on the relaxation spectrum of shorter and therefore stiffer alkane chains in a melt.

***

This investigation is part of a project of the Sonderforschungbereich 239. The support of the Deutsche Forschungsgemeinschaft is gratefully acknowledged.

REFERENCES

[1] Rouse P. E., *J. Chem. Phys.*, **21** (1953) 1272.
[2] de Gennes P. G., *Physics (Long Island City, N. Y.)*, **3** (1967) 37.
[3] Akcasu A. Z., Benmouna M. and Han C. C., *Polymer*, **21** (1980) 866.
[4] Doi M. and Edwards S. F., *The Theory of Polymer Dynamics*, (Clarendon, Oxford) 1986.
[5] Richter D., Ewen B., Farago B. and Wagner T., *Phys. Rev. Lett.*, **18** (1989) 2140.
[6] Paul W., Smith G. D. and Yoon D. Y., *Macromolecules*, **30** (1997) 7772.
[7] Paul W., Smith G. D., Yoon D. Y., Farago B., Rathgeber S., Zirkel A., Willner L. and Richter D., *Phys. Rev. Lett*, **80** (1998) 2346.
[8] Kostov K. S., Freed K. F., Webb E. B., Mondello M. and Grest G. S., *J. Chem. Phys.*, **108** (1998) 9155.

[9] Mondello M., Grest G. S., Webb E. B. and Peczak P., *J. Chem. Phys.*, **109** (1998) 798.
[10] Winkler R. G., Reineker P. and Harnau L., *J. Chem. Phys.*, **101** (1994) 8119.
[11] Harnau L., Winkler R. G. and Reineker P., *J. Chem. Phys.*, **106** (1997) 2469.
[12] Harnau L., *Zur Theorie dynamischer und statischer Strukturfaktoren von Makromolekülen unterschiedlicher Molekülsteifigkeit*, Dissertation (Cuviller, Göttingen) 1998.
[13] Yamakawa H., *Ann. Rev. Phys. Chem.*, **35** (1984) 23.
[14] Paul W., Yoon D. Y. and Smith G. D., *J. Chem. Phys.*, **103** (1995) 1702.
[15] Aragón S. R. and Pecora R., *Macromolecules*, **18** (1985) 1868.
[16] Binder K. and Paul W., *J. Polym. Sci. Part B: Polym. Phys.*, **35** (1997) 1.
[17] Granek R., *J. Phys. II*, **7** (1997) 1761.
[18] Caspi A., Elbaum M., Granek R., Lachish A. and Zbaida D., *Phys. Rev. Lett.*, **80** (1998) 1106.
[19] Farge E. and Maggs A. C., *Macromolecules*, **26** (1993) 5041.
[20] Götter R., Kroy K., Frey E., Bärmann M. and Sackmann E., *Macromolecules*, **29** (1996) 30.
[21] Kroy K. and Frey E., *Phys. Rev. E*, **55** (1997) 3092.